Available online at www.sciencedirect.com
SCIENCE DIRECT®
Physica B 335 (2003) 82–88
PHYSICA B
www.elsevier.com/locate/physb

Simulations of off-specular scattering of polarized neutrons from laterally patterned magnetic multilayers

E. Kentzinger[a,*], U. Rücker[a], B.P. Toperverg[a,b]

[a] *Institut für Festkörperforschung, Forschungszentrum Jülich, D-52425 Jülich, Germany*
[b] *Petersburg Nuclear Physics Institute, Gatchina, 188350 St. Petersburg, Russia*

Abstract

We put forward a new presentation of the theory of off-specular scattering of polarized neutrons from magnetic multilayers within the distorted wave Born approximation developed by one of the authors. In this presentation, a clear separation is made between (1) the structure factors, model dependent, and (2) the optical coefficients and the efficiencies of the polarizer and the analyzer, model independent. It therefore permits an easy plugging in of any particular model of structural and magnetic correlations. For a test, we show simulations of off-specular scattering from magnetic domains in multilayers exhibiting anti-ferromagnetic coupling, a situation encountered in the literature.

PACS: 75.25.+z; 75.70.Kw; 75.75.+a

Keywords: Magnetic thin films; Magnetoelectronics; Off-specular scattering of polarized neutrons

1. Introduction

The magnetoelectronic properties of multilayers are usually interpreted in the framework of models considering those structures as laterally invariant. However, the effect of structural roughness and magnetic domains has already been pointed out, e.g. the case of the giant magnetoresistance effect [1,2]. Usual techniques to study those inhomogeneities, such as scanning tunnel microscopy, magnetic force microscopy (MFM) or scanning electron microscopy with polarization analysis are surface or near-surface techniques that do not give any information on the buried layers and interfaces. For example, MFM is a technique that monitors the stray fields above the surface. In the case of thin films showing perpendicular magnetic anisotropy, it hardly gives any access to the closure domains inside the sample [3].

Scattering of X-rays and neutrons at grazing incidence can give access to informations on the buried layers, see e.g. Refs. [4,5]. The analysis of magnetic scattering at grazing incidence is not an easy task and, in the case of neutrons, has received only recently a full theoretical description in the framework of the distorted wave Born approximation (DWBA), by one of the authors [6–8]. This description allows to simulate the reflectivity and off-specular scattering of polarized neutron for any structural or magnetization arrangement, as long as a statistical description of it can be provided, and for any directions of incident polarization and polarization analysis.

*Corresponding author. Fax: +49-2461-61-2610.
E-mail address: e.kentzinger@fz-juelich.de (E. Kentzinger).

0921-4526/03/$ - see front matter
doi:10.1016/S0921-4526(03)00213-8

We put forward a new presentation of this description, in which the model-dependent contributions, i.e. the Fourier transforms of the correlations, are clearly separated from the model-independent contributions, i.e. the optical coefficients and the polarizer and analyzer efficiencies. For a test, we performed simulations considering the situation studied by Lauter-Pasyuk et al. [5] and Toperverg et al. [9] of a multilayer with magnetic domains and anti-ferromagnetic coupling within the domains.

2. Off-specular scattering of polarized neutrons in the DWBA

2.1. The Hamiltonian

Let us consider a neutron beam impinging on the multilayer surface with incident angle α_i and wave vector $\mathbf{k}_i$ and a detection system measuring the scattered neutrons with wave vector $\mathbf{k}_f$ in a solid angle $d\Omega$, centered around the direction defined by the exit and azimuth angles α_f and ϕ_f, respectively. The stationary states of scattering are solutions of the stationary Schrödinger wave equation:

$$\hat{H}|\psi(\mathbf{r})\rangle = E|\psi(\mathbf{r})\rangle \quad \text{with } E = \frac{\hbar^2 k^2}{2m}. \tag{1}$$

In the case of a magnetic multilayer, the Hamiltonian operator can be written as

$$\hat{H} = -\frac{\hbar^2}{2m}\hat{I}\Delta + \sum_m \hat{V}_m(\mathbf{r}), \quad \text{where}$$
$$\hat{V}_m(\mathbf{r}) = V_m^N(\mathbf{r})\hat{I} - \hat{\boldsymbol{\mu}}\mathbf{B}_m(\mathbf{r}) \tag{2}$$

is the interaction potential operator in layer m, $V_m^N(\mathbf{r})$ is the nuclear interaction potential, $\mathbf{B}_m(\mathbf{r})$ is the magnetic induction, $\hat{\boldsymbol{\mu}} = \mu\hat{\boldsymbol{\sigma}}$ is the neutron magnetic moment operator, $\hat{I}$ is the 2×2 unit matrix, and $\hat{\boldsymbol{\sigma}} = (\hat{\sigma}_x, \hat{\sigma}_y, \hat{\sigma}_z)$ is the vector of the Pauli matrices. The eigenvectors

$$|\chi^+\rangle = \begin{pmatrix} 1 \\ 0 \end{pmatrix} \quad \text{and } |\chi^-\rangle = \begin{pmatrix} 0 \\ 1 \end{pmatrix} \tag{3}$$

of the matrix $\hat{\sigma}_z$ define states of the neutron with "+" or "−" spin projections. If the z-axis is chosen (for example, along $\mathbf{B}_m$), then the neutron wave function

$$|\psi(\mathbf{r})\rangle = \psi^+(\mathbf{r})|\chi^+\rangle + \psi^-(\mathbf{r})|\chi^-\rangle = \begin{pmatrix} \psi^+(\mathbf{r}) \\ \psi^-(\mathbf{r}) \end{pmatrix} \tag{4}$$

is given by the pair of functions $\psi^{\pm}(\mathbf{r})$ depending on the choice.

2.2. The DWBA

Let us now consider that the potential operator in each layer can be decomposed in the form:

$$\hat{V}_m(\mathbf{r}) = \hat{V}_m^{av}(z) + \hat{V}_m^{pert}(\mathbf{r}), \tag{5}$$

where $\hat{V}_m^{av}(z) = \langle \hat{V}_m(\mathbf{r})\rangle_{\boldsymbol{\rho}}$ is an average of the potential over all lateral coordinates $\boldsymbol{\rho}$ (i.e. parallel to the surface) and depends only on the coordinate z perpendicular to the surface. $\hat{V}_m^{av}(z)$ leads to the specular reflectivity. The second term $\hat{V}_m^{pert}(\mathbf{r})$ is responsible for the off-specular scattering. From a Born development to first order in $\hat{V}_m$ of the integral equation of scattering, it can be shown that if $\hat{V}_m^{pert}$ is small with respect to $\hat{V}_m^{av}$, the differential scattering cross section for off-specular scattering can be written as [7,8,10]:

$$\frac{d\sigma}{d\Omega} = \overline{\left|\sum_m \langle \widetilde{\psi^{av}_{\mathbf{k}_f}}|\hat{V}_m^{pert}|\psi^{av}_{\mathbf{k}_i}\rangle\right|^2}, \tag{6}$$

where $|\psi^{av}_{\mathbf{k}_i}\rangle$ and $|\widetilde{\psi^{av}_{\mathbf{k}_f}}\rangle$ are the solutions of the stationary Schrödinger equation for the reference potential $\hat{\mathbf{V}}_m^{av}(z)$ for neutrons impinging with wave vectors $\mathbf{k}_i$ and $-\mathbf{k}_f$, respectively. The line above this equation stands for an average over the initial states that are prepared by the polarizer and over the final states that are accepted by the analyzer. This cross section has the same form as a scattering cross section in the Born approximation, except that the matrix element is taken between brackets that represent states that are "distorted" by the reference potential $\hat{\mathbf{V}}_m^{av}$. This is why this approximation is called the DWBA [10], which was used by many authors to simulate, for example, surface diffraction [11,12] and off-specular scattering from structural roughness [13].

2.3. The reference states and the reflectivity

The reference states can be evaluated exactly. The reference Hamiltonian is independent of the lateral coordinate $\boldsymbol{\rho}$. Therefore, the reference state in layer m can be written as

$$|\psi_m^{\mathrm{av}}(\mathbf{r})\rangle = \exp(\mathrm{i}\boldsymbol{\kappa}\boldsymbol{\rho})|\psi_m^{\mathrm{av}}(z)\rangle, \tag{7}$$

where $\boldsymbol{\kappa}$ is the in-plane (conserving) projection of the wave vector $\mathbf{k}$, and

$$|\psi_m^{\mathrm{av}}(z)\rangle = \hat{S}^m(z)|\psi_m^{\mathrm{av}}(0)\rangle \quad \text{with}$$
$$\hat{S}^m(z) = \mathrm{e}^{\mathrm{i}\hat{\varphi}_m(z)}\hat{t}_m + \mathrm{e}^{-\mathrm{i}\hat{\varphi}_m(z)}\hat{r}_m. \tag{8}$$

$\hat{S}^m(z)$ is the propagation operator, $\hat{t}_m$ and $\hat{r}_m$ are the operators of transmission and reflection amplitudes in layer m, $\hat{\varphi}_m(z) = \hat{p}_m(z - z_{m-1})$, where $\hat{p}_m = \sqrt{p_0^2 - \hat{p}_{mc}^2}$ is the z-component of the wave vector operator in layer m and $p_0 = \sqrt{k^2 - \kappa^2}$ is the z component of the wave vector in vacuum. Like any 2×2 matrix, $\hat{p}_m$ can be written as a linear combination of the unit matrix and the Pauli matrices:

$$\hat{p}_m = \tfrac{1}{2}\{(p_m^+ + p_m^-)\hat{1} + (\hat{\boldsymbol{\sigma}}\mathbf{b}_m)(p_m^+ - p_m^-)\}. \tag{9}$$

$p_m^{\pm}$ are the eigenvalues of $\hat{p}_m$: $p_m^{\pm} = \sqrt{p_0^2 - p_{mc}^{\pm 2}}$ with $p_{mc}^{\pm 2} = 4\pi(\overline{\mathrm{nb}_m^{\mathrm{N}}} \mp \overline{\mathrm{nb}_m^{\mathrm{M}}})$, where $\overline{\mathrm{nb}_m^{\mathrm{N}}}$ and $\overline{\mathrm{nb}_m^{\mathrm{M}}}$ are the lateral averages of the nuclear and magnetic scattering length densities in layer m. $\mathbf{b}_m = \mathbf{B}_m/|\mathbf{B}_m|$.

The operators of reflection and transmission amplitudes in each layer can be deduced recursively from the continuity conditions at all interfaces of the wave function and its derivative with respect to z, in the same way as the one used by Parratt [14]. For the sake of completeness of this article, those operators are derived in Appendix A.

The reflectivity can also be evaluated from the reflectance matrix $\hat{\mathbf{R}} = \hat{\mathbf{r}}_{\mathbf{0}}$. The measured reflectivity is defined by the relation:

$$\mathscr{R} = \overline{|\langle\psi_{0,\mathrm{f}}^{\mathrm{av}}(0)|\hat{R}|\psi_{0,\mathrm{i}}^{\mathrm{av}}(0)\rangle|^2} = \mathrm{Tr}\{\hat{\rho}_{\mathrm{f}}\hat{R}\hat{\rho}_{\mathrm{i}}\hat{R}^+\}, \tag{10}$$

where $\hat{\rho}_{\mathrm{i}}$ and $\hat{\rho}_{\mathrm{f}}$ are the density matrices of the polarizer and the analyzer, respectively: $\hat{\rho}_{\mathrm{i,f}} = \frac{1}{2}(\hat{I} + \mathbf{P}_{\mathrm{i,f}}\hat{\boldsymbol{\sigma}})$, $\mathbf{P}_{\mathrm{i}}$ and $\mathbf{P}_{\mathrm{f}}$ being the polarization and analysis vectors, respectively.

2.4. Off-specular scattering

We are now able to calculate the scattering cross section for off-specular scattering. Eq. (6) can be written in the following way:

$$\frac{\mathrm{d}\sigma}{\mathrm{d}\Omega} = \overline{\left|\sum_m \langle\widetilde{\psi_{\mathbf{k}_{\mathrm{f}}}^{\mathrm{av}}}(0)|\hat{S}_{\mathrm{f}}^m\hat{V}_m^{\mathrm{pert}}\hat{S}_{\mathrm{i}}^m|\psi_{\mathbf{k}_{\mathrm{i}}}^{\mathrm{av}}(0)\rangle\right|^2}$$
$$= \sum_{m,m'}\mathrm{Tr}(\hat{\rho}_{\mathrm{i}}\hat{F}_{\mathrm{fi}}^{m+}\hat{\rho}_{\mathrm{f}}\hat{F}_{\mathrm{fi}}^{m'}) \tag{11}$$

with

$$\hat{F}_{\mathrm{fi}}^m = \int \mathrm{d}\boldsymbol{\rho}\,\mathrm{e}^{\mathrm{i}\mathbf{Q}_\parallel\boldsymbol{\rho}}\int_{z_{m-1}}^{z_m}\mathrm{d}z\,\hat{S}_{\mathrm{f}}^m(z)\hat{V}_m^{\mathrm{pert}} \times (\boldsymbol{\rho}, z)\hat{S}_{\mathrm{i}}^{\mathrm{m}}(z), \tag{12}$$

$$\hat{S}_{\mathrm{i}}^m(z) = \mathrm{e}^{\mathrm{i}\hat{p}_{m\mathrm{i}}z}\hat{t}_{m\mathrm{i}} + \mathrm{e}^{-\mathrm{i}\hat{p}_{m\mathrm{i}}z}\hat{r}_{m\mathrm{i}}, \tag{13}$$

$$\hat{S}_{\mathrm{f}}^m(z) = \hat{t}_{m\mathrm{f}}\,\mathrm{e}^{\mathrm{i}\hat{p}_{m\mathrm{f}}z} + \hat{r}_{m\mathrm{f}}\,\mathrm{e}^{-\mathrm{i}\hat{p}_{m\mathrm{f}}z} \tag{14}$$

and where $\hat{F}_{\mathrm{fi}}^{m+}$ is the hermitian conjugate of $\hat{F}_{\mathrm{fi}}^m$. $\mathbf{Q}_\parallel$ is the in-plane component of the scattering wave vector $\mathbf{Q} = \mathbf{k}_{\mathrm{f}} - \mathbf{k}_{\mathrm{i}}$. Combining Eqs. (11), (8) and (2) one can obtain the final result:

$$\frac{\mathrm{d}\sigma}{\mathrm{d}\Omega} = \frac{\mathrm{d}\sigma}{\mathrm{d}\Omega}^{\mathrm{NN}} + \frac{\mathrm{d}\sigma}{\mathrm{d}\Omega}^{\mathrm{NM}} + \frac{\mathrm{d}\sigma}{\mathrm{d}\Omega}^{\mathrm{MN}} + \frac{\mathrm{d}\sigma}{\mathrm{d}\Omega}^{\mathrm{MM}}. \tag{15}$$

The first term on the right-hand side of this equation gives the diffuse scattering from the nuclear–nuclear correlations, the two following ones describe scattering from the nuclear–magnetic correlations and the last one scattering from the magnetic–magnetic correlations.

$$\frac{\mathrm{d}\sigma}{\mathrm{d}\Omega}^{\mathrm{NN}} = J_{\mu\nu\ \mu'\nu'}^{m\alpha\beta m'\alpha'\beta'}K_{\mathrm{NN}}^{mm'}(q_{\mu\nu}^{m\alpha\beta}, q_{\mu'\nu'}^{m'\alpha'\beta'}, \mathbf{Q}_\parallel),$$
$$\frac{\mathrm{d}\sigma}{\mathrm{d}\Omega}^{\mathrm{NM}} = J_{\lambda\ \mu\nu\ \mu'\nu'}^{\ m\alpha\beta m'\alpha'\beta'}K_{\mathrm{NM}}^{\lambda,mm'}(q_{\mu\nu}^{m\alpha\beta}, q_{\mu'\nu'}^{m'\alpha'\beta'}, \mathbf{Q}_\parallel),$$
$$\frac{\mathrm{d}\sigma}{\mathrm{d}\Omega}^{\mathrm{MN}} = \tilde{J}_{\lambda\ \mu\nu\ \mu'\nu'}^{\ m\alpha\beta m'\alpha'\beta'}K_{\mathrm{MN}}^{\lambda,mm'}(q_{\mu\nu}^{m\alpha\beta}, q_{\mu'\nu'}^{m'\alpha'\beta'}, \mathbf{Q}_\parallel),$$
$$\frac{\mathrm{d}\sigma}{\mathrm{d}\Omega}^{\mathrm{MM}} = J_{\lambda\lambda'\ \mu\nu\ \mu'\nu'}^{\ m\alpha\beta m'\alpha'\beta'}K_{\mathrm{MM}}^{\lambda\lambda',mm'}(q_{\mu\nu}^{m\alpha\beta}, q_{\mu'\nu'}^{m'\alpha'\beta'}, \mathbf{Q}_\parallel). \tag{16}$$

The J coefficients depend only on the optical constants and on the efficiencies of the polarizer

and the analyzer:

$$
\begin{aligned}
J^{m\alpha\beta m'\alpha'\beta'}_{\mu\nu\ \ \mu'\nu'} &= \mathrm{Tr}\{\hat{\rho}_\mathrm{i}[\hat{N}^{m\alpha\beta}_{\mu\nu}]^+\hat{\rho}_\mathrm{f}\hat{N}^{m'\alpha'\beta'}_{\mu'\nu'}\},\\
J^{m\alpha\beta m'\alpha'\beta'}_{\lambda\ \ \mu\nu\ \ \mu'\nu'} &= \mathrm{Tr}\{\hat{\rho}_\mathrm{i}[\hat{N}^{m\alpha\beta}_{\mu\nu}]^+\hat{\rho}_\mathrm{f}\hat{M}^{m'\alpha'\beta'}_{\lambda\ \ \mu'\nu'}\},\\
\tilde{J}^{m\alpha\beta m'\alpha'\beta'}_{\lambda\ \ \mu\nu\ \ \mu'\nu'} &= \mathrm{Tr}\{\hat{\rho}_\mathrm{i}[\hat{M}^{m\alpha\beta}_{\lambda\ \ \mu\nu}]^+\hat{\rho}_\mathrm{f}\hat{N}^{m'\alpha'\beta'}_{\mu'\nu'}\},\\
J^{m\alpha\beta m'\alpha'\beta'}_{\lambda\lambda'\ \ \mu\nu\ \ \mu'\nu'} &= \mathrm{Tr}\{\hat{\rho}_\mathrm{i}[\hat{M}^{m\alpha\beta}_{\lambda\ \ \mu\nu}]^+\hat{\rho}_\mathrm{f}\hat{M}^{m'\alpha'\beta'}_{\lambda'\ \ \mu'\nu'}\}
\end{aligned}
\tag{17}
$$

with

$$
\begin{aligned}
\hat{N}^{m\alpha\beta}_{\mu\nu} &= \hat{A}^{m\alpha}_\mathrm{f}\hat{\Lambda}^m_\mu\hat{\Lambda}^m_\nu\hat{A}^{m\beta}_\mathrm{i},\\
\hat{M}^{m\alpha\beta}_{\lambda\ \ \mu\nu} &= \hat{A}^{m\alpha}_\mathrm{f}\hat{\Lambda}^m_\mu\hat{\sigma}_\lambda\hat{\Lambda}^m_\nu\hat{A}^{m\beta}_\mathrm{i},
\end{aligned}
$$

where

$$
\hat{\Lambda}^m_\pm = 1/2[\hat{1}\pm(\hat{\boldsymbol{\sigma}}\mathbf{b}_m)]. \tag{18}
$$

The notation in Eq. (16) implies summations over all indices:

- m, m' are layer indices,
- $\hat{A}^{m\alpha} = \hat{t}_m$ and $\hat{r}_m$ for $\alpha,\beta = 1$ and 2, respectively,
- μ,ν take the values $+1$ and -1,
- λ,λ' stand for the indices x, y and z.

$$
\begin{aligned}
q^{mtt}_{\mu\nu} &= p^\mu_{m\mathrm{f}} + p^\nu_{m\mathrm{i}} = -q^{mrr}_{\mu\nu},\\
q^{mtr}_{\mu\nu} &= p^\mu_{m\mathrm{f}} - p^\nu_{m\mathrm{i}} = -q^{mrt}_{\mu\nu}.
\end{aligned}
\tag{19}
$$

The structure factors in Eq. (16) are Fourier transforms of correlation functions:

$$
\begin{aligned}
&K^{mm'}_\mathrm{NN}(q,q',\mathbf{Q}_\parallel)\\
&\quad= \mathscr{N}_0\mathscr{S}_\mathrm{coh}\int \mathrm{d}\boldsymbol{\rho}\,\mathrm{e}^{\mathrm{i}\mathbf{Q}_\parallel\boldsymbol{\rho}}\int_0^{d_m}\mathrm{d}z\,\mathrm{e}^{-\mathrm{i}q^+z}\int_0^{d_{m'}}\mathrm{d}z'\,\mathrm{e}^{\mathrm{i}q'z'}\\
&\qquad\times\langle\Delta\mathrm{nb}^\mathrm{N}_m(z,\boldsymbol{\rho})\Delta\mathrm{nb}^\mathrm{N}_{m'}(z',0)\rangle,\\
&K^{\lambda,mm'}_\mathrm{NM}(q,q',\mathbf{Q}_\parallel)\\
&\quad= \mathscr{N}_0\mathscr{S}_\mathrm{coh}\int \mathrm{d}\boldsymbol{\rho}\,\mathrm{e}^{\mathrm{i}\mathbf{Q}_\parallel\boldsymbol{\rho}}\int_0^{d_m}\mathrm{d}z\,\mathrm{e}^{-\mathrm{i}q^+z}\int_0^{d_{m'}}\mathrm{d}z'\,\mathrm{e}^{\mathrm{i}q'z'}\\
&\qquad\times\langle\Delta\mathrm{nb}^\mathrm{N}_m(z,\boldsymbol{\rho})\Delta\mathrm{nb}^{\mathrm{M},\lambda}_{m'}(z',0)\rangle,\\
&K^{\lambda,mm'}_\mathrm{MN}(q,q',\mathbf{Q}_\parallel)\\
&\quad= \mathscr{N}_0\mathscr{S}_\mathrm{coh}\int \mathrm{d}\boldsymbol{\rho}\,\mathrm{e}^{\mathrm{i}\mathbf{Q}_\parallel\boldsymbol{\rho}}\int_0^{d_m}\mathrm{d}z\,\mathrm{e}^{-\mathrm{i}q^+z}\int_0^{d_{m'}}\mathrm{d}z'\,\mathrm{e}^{\mathrm{i}q'z'}\\
&\qquad\times\langle\Delta\mathrm{nb}^{\mathrm{M},\lambda}_m(z,\boldsymbol{\rho})\Delta\mathrm{nb}^\mathrm{N}_{m'}(z',0)\rangle,
\end{aligned}
$$

$$
\begin{aligned}
&K^{\lambda\lambda',mm'}_\mathrm{MM}(q,q',\mathbf{Q}_\parallel)\\
&\quad= \mathscr{N}_0\mathscr{S}_\mathrm{coh}\int \mathrm{d}\boldsymbol{\rho}\,\mathrm{e}^{\mathrm{i}\mathbf{Q}_\parallel\boldsymbol{\rho}}\int_0^{d_m}\mathrm{d}z\,\mathrm{e}^{-\mathrm{i}q^+z}\int_0^{d_{m'}}\mathrm{d}z'\,\mathrm{e}^{\mathrm{i}q'z'}\\
&\qquad\times\langle\Delta\mathrm{nb}^{\mathrm{M},\lambda}_m(z,\boldsymbol{\rho})\Delta\mathrm{nb}^{\mathrm{M},\lambda'}_{m'}(z',0)\rangle.
\end{aligned}
\tag{20}
$$

In those equations, $\Delta\mathrm{nb}^\mathrm{N}_m(z,\boldsymbol{\rho})$ is the nuclear scattering length density fluctuation and $\Delta\mathrm{nb}^{\mathrm{M},\lambda}_m(z,\boldsymbol{\rho})$ is the projection of the magnetic scattering length density fluctuation along the axis λ. The brackets stand for averages over all possible origins of the lateral coordinate $\boldsymbol{\rho}$ on the surface $\mathscr{S}_\mathrm{coh}$ of coherent illumination by the neutron beam. $\mathscr{N}_0$ is a number such that the surface of the sample illuminated by the beam equals $\mathscr{N}_0\mathscr{S}_\mathrm{coh}$. d_m is the thickness of layer m. $q = q^{m\alpha\beta}_{\mu\nu}$ and $q^+ = (q^{m\beta\alpha}_{\nu\mu})^*$.

Important to note is that all the scattering cross sections in Eq. (16) are sums of products of two different types of terms. One type depends only on the optical coefficients and on the analyzer and polarizer characteristics. The other one is a Fourier transform of the correlation functions. This presentation is therefore very general. The only system-dependent part lies in the decomposition of the interaction potential in Eq. (5) and in the calculation of the structure factors in Eq. (20).

In the following section, we give an example of the application of this formalism in the case of multilayers with magnetic domains. In another article of this volume [15], the same model as below is used to fit experimental data.

3. Magnetic domains

Let us consider the situation depicted in Fig. 1 and already considered in Refs. [5,9]. The authors of this study obtained this situation in an Fe/Cr multilayer with a fourfold magnetic anisotropy (easy axis of magnetization along x and y) and anti-ferromagnetic (AF) coupling between the Fe layers. This peculiar magnetization distribution was obtained by reducing the magnetic field H applied along the y-axis, starting from the saturated state. The mean magnetization in each layer is directed along the field. This mean magnetization, whose norm is $M_m\sin(\Phi)$,

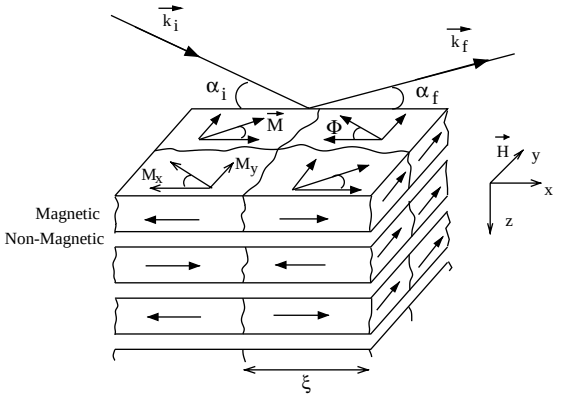

Fig. 1. Model of domains in a multilayer with anti-ferromagnetic coupling between the ferromagnetic layers. See the text for more details.

contributes to the specular reflectivity, while the components of the magnetic moments along the x-axis cause the diffuse scattering.

To increase the generality of the latter model and for the purpose of simulating experimental data presented in another article of this volume [15], we consider here a model in which the angle to the x-axis, that we will now call φ, can fluctuate randomly from domain to domain around Φ. In that case, both the x and y components of the magnetizations will contribute to the diffuse scattering.

In this situation, only the K_{MM}^{xx} and K_{MM}^{yy} elements in (20) are non-equal to zero. After averaging over Q_y, one has

$$K_{\mathrm{MM}}^{\lambda\lambda',mm'}(q,q',Q_x) = \mathscr{N}_0 \mathscr{S}_{\mathrm{coh}} 2\pi \overline{\mathrm{nb}_m^{\mathrm{M}}}\,\overline{\mathrm{nb}_{m'}^{\mathrm{M}}} \times W_{mm'}^{\lambda\lambda'}(Q_x) G_m(q^+) G'_{m'}(q) \quad (21)$$

with

$$W_{mm'}^{xx}(Q_x) = \frac{C_{mm'}\xi}{(Q_x\xi)^2+1}, \quad \text{where}$$

$$C_{mm'} = \langle \cos(\varphi_m)\cos(\varphi_{m'})\rangle,$$

$$W_{mm'}^{yy}(Q_x) = \frac{S_{mm'}\xi}{(Q_x\xi)^2+1}, \quad \text{where}$$

$$S_{mm'} = \langle \sin(\varphi_m)\sin(\varphi_{m'})\rangle - \langle \sin(\varphi_m)\rangle^2 \delta_{mm'} \quad (22)$$

and

$$G_m(q^+) = \frac{\mathrm{e}^{-\mathrm{i}q_m^+ d_m} - 1}{-\mathrm{i}q_m^+},$$

$$G'_{m'}(q) = \frac{\mathrm{e}^{\mathrm{i}q_{m'} d_{m'}} - 1}{\mathrm{i}q_{m'}}. \quad (23)$$

ξ is the average size of a domain. In the same way as in Ref. [13], the Q_x dependency of the structure factors $W_{mm'}^{\lambda\lambda'}$ is deduced assuming that the fluctuations can be described in terms of fractal Brownian motion [16].

The φ_m's as randomly fluctuating quantities obey a Gaussian statistics. Let us call σ its root-mean-square width. Then, the correlations within one layer are

$$C_{mm} = \frac{1}{2}\{1 + \cos(2\Phi)\mathrm{e}^{-2\sigma^2}\},$$

$$S_{mm} = \frac{1}{2}\{1 - \cos(2\Phi)\mathrm{e}^{-\sigma^2}\}\{1 - \mathrm{e}^{-\sigma^2}\}. \quad (24)$$

To take into account the AF correlations between two nearest-neighbor ferromagnetic layers, one can write, as a simplest model, $C_{mm'} = C_{mm}(-1)^{|m-m'|/2}\,\mathrm{e}^{-|m-m'|/m_0}$ and $S_{mm'} = 0$. The bigger m_0, the stronger the vertical correlations.

In the top picture of Fig. 2, we show a simulation of spin-flip diffuse scattering in the special case considered by Lauter-Pasyuk et al. [5] and Toperverg et al. [9], i.e. for a polarization and a polarization analysis along y, without fluctuations ($\sigma = 0$), and with vertically correlated domains (m_0 big with respect to the number of layers). The intensity variation along the diagonal is highly modulated, due to the vertical correlations. Perpendicular to this diagonal, the width of the peaks are inversely proportional to ξ, the average size of the domains. The intensity has maxima at the positions of AF Bragg reflections. However, no intensity is seen at the structural Bragg reflections. This is because (1) no fluctuation along the y-axis is considered and (2) spin-flip scattering is simulated. Another interesting feature in this picture is the asymmetry in the intensity distribution. The asymmetry is the most pronounced for α_i and α_f close to the total reflection edges. This can be explained, in the framework of the DWBA, by the fact that the scattering is modulated by some combinations of the reflection

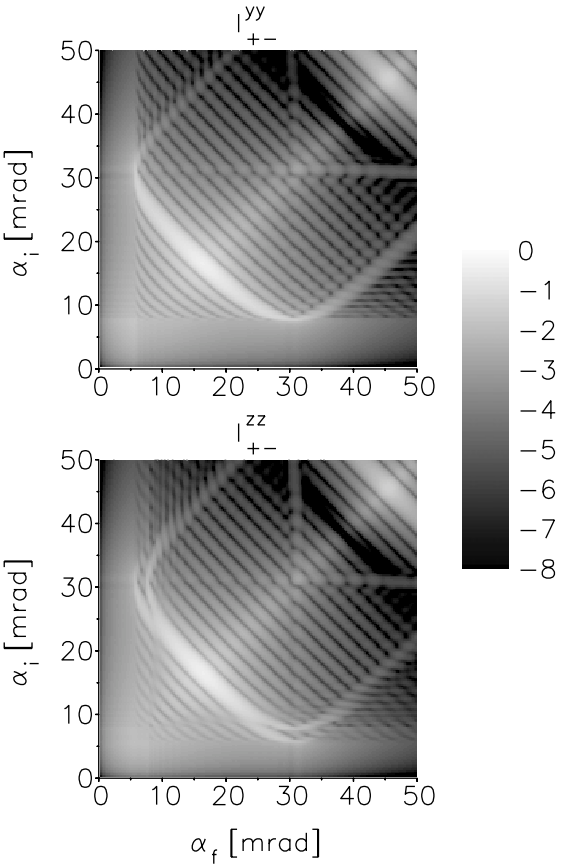

Fig. 2. (a) Simulations of spin-flip diffuse scattering of polarized neutrons from an $[Fe(60\ Å)/Cr(15\ Å)]_{20}$ multilayer exhibiting anti-ferromagnetic coupling, with magnetic domains. In the top example, the directions of incident polarization and analysis lie along the y-axis of (b). The same geometry was considered in Ref. [9]. In the bottom one, spin-flip scattering is also considered, but the directions of polarization and analysis lie along the z-axis. Intensities are displayed on a logarithmic scale. ($\lambda = 4.5$ Å, $\xi = 1$ μm, $\Phi = 30°$, $\sigma = 0$ and m_0 very big with respect to the number of layers.)

and transmission amplitudes (J-coefficients in the cross sections of Eq. (16)) and that those amplitudes have maxima at the critical angles of total reflection. The critical angle of total reflection of spin-up neutrons (incoming ones) is bigger than the critical angle for spin-down neutrons (the one selected by the analyzer). This asymmetry appeared in the data of Ref. [5] and were discussed in Ref. [17].

In the bottom picture of Fig. 2, we consider the same magnetic arrangement as above, spin-flip scattering also, but with the directions of polarization and analysis along the z-axis (situation not considered in Refs. [5,9]). The intensity variations are the same as above, except for the weighting by refraction effects. Due to the fact that spin-up and spin-down neutrons see the same mean potential, the intensity distribution is, in that case, symmetrical, with an enhancement of the intensity at the two critical angles of total reflection for spin-up and spin-down neutrons.

4. Conclusion

We have given a new presentation of the formalism of off-specular scattering of polarized neutrons with polarization analysis developed by one of the authors. A clear separation is made between (1) the structure factors, model dependent, and (2) the optical coefficients and the efficiencies of the polarizer and the analyzer, model independent. As a test of its implementation, we performed simulations in the case already encountered in the literature of domains in anti-ferromagnetically coupled multilayers.

Appendix A. Operators of reflection and transmission amplitudes

The operators $\hat{t}_m$ and $\hat{r}_m$ of transmission and reflection amplitudes in layer m were defined in Eq. (8). The conditions of continuity of the wave function and its first derivative with respect to z at each interface z_m impose that

$$\begin{aligned} &e^{i\hat{\varphi}_m}\hat{t}_m + e^{-i\hat{\varphi}_m}\hat{r}_m = \hat{t}_{m+1} + \hat{r}_{m+1}, \\ &\hat{p}_m(e^{i\hat{\varphi}_m}\hat{t}_m - e^{-i\hat{\varphi}_m}\hat{r}_m) = \hat{p}_{m+1}(\hat{t}_{m+1} - \hat{r}_{m+1}) \end{aligned} \qquad \text{(A.1)}$$

with $\hat{\varphi}_m = \hat{p}_m(z_m - z_{m-1}) = \hat{p}_m d_m$, where d_m is the thickness of layer m. In vacuum $\hat{t}_0 = \hat{1}$ and $\hat{r}_0 = \hat{R}$ (the reflectance matrix) and, in the substrate, $\hat{t}_{N+1} = \hat{T}$ (the transmittance matrix) and $\hat{r}_{N+1} = \hat{0}$, N being the number of layers. Defining $\hat{X}_m = (\hat{r}_m\hat{t}_m^{-1})$, one can show that $\hat{X}_m = e^{i\hat{\varphi}_m}\tilde{X}_m e^{i\hat{\varphi}_m}$

with

$$\hat{\tilde{X}}_m = \{(\hat{1} - \hat{p}_m^{-1}\hat{p}_{m+1}) + (\hat{1} + \hat{p}_m^{-1}\hat{p}_{m+1})\hat{X}_{m+1}\} \times \{(\hat{1} + \hat{p}_m^{-1}\hat{p}_{m+1}) + (\hat{1} - \hat{p}_m^{-1}\hat{p}_{m+1})\hat{X}_{m+1}\}^{-1}. \quad (A.2)$$

Starting from $\hat{X}_{N+1} = 0$, the $\hat{X}_m$ coefficients can be obtained recursively by iterating m down to 0. $\hat{X}_0$ equals the reflection amplitude into vacuum $\hat{R}$. The operators of reflection and transmission amplitudes in each layer m can afterwards be recursively deduced, starting from $m = 0$ and iterating m up to N:

$$\hat{r}_m = \hat{X}_m \hat{t}_m,$$

$$\hat{t}_{m+1} = \{\hat{1} + \hat{X}_{m+1}\}^{-1}\{\hat{1} + \hat{\tilde{X}}_m\} e^{i\hat{\varphi}_m} \hat{t}_m. \quad (A.3)$$

This formulation of the amplitudes allowed us to simulate polarized neutron reflectivity and off-specular scattering of systems consisting of a large amount of layers, like supermirrors [18], without any numerical problem like numbers getting too big. The reason is that all the arguments in the complex exponentials have *positive* imaginary parts, leading to complex exponentials having norm smaller than 1. This is not the case for the reflection and transmission amplitudes calculated within the "supermatrix" formalism [19,20,8].

The amplitudes $\hat{t}_{mi}$ and $\hat{r}_{mi}$ as defined in Eq. (13) were deduced using the above formula. Similar formula can be obtained for the amplitudes $\hat{t}_{mf}$ and $\hat{r}_{mf}$ as defined in Eq. (14).

References

[1] D. Olligs, D.E. Bürgler, Y.G. Wang, E. Kentzinger, U. Rücker, R. Schreiber, Th. Brückel, P. Grünberg, Europhys. Lett. 59 (2000) 459.
[2] M. Hehn, O. Lenoble, D. Lacour, C. Féry, M. Piécuch, C. Tiusan, K. Ounadjela, Phys. Rev. B 61 (2000) 11643.
[3] V. Gehanno, A. Marty, B. Gilles, Y. Samson, Phys. Rev. B 55 (1997) 12552.
[4] H.A. Dürr, E. Dudzik, S.S. Dhesi, J.B. Goedkoop, G. van der Laan, M. Belakhovsky, C. Mocuta, A. Marty, Y. Samson, Science 284 (1999) 2166.
[5] V. Lauter-Pasyuk, H.J. Lauter, B. Toperverg, O. Nikonov, E. Kravtsov, M.A. Milyaev, L. Romashev, V. Ustinov, Physica B 283 (2000) 194.
[6] B.P. Toperverg, Physica B 297 (2001) 160.
[7] B.P. Toperverg, in: Th. Brückel, W. Schweika (Eds.), Polarized neutron reflection and off-specular scattering, in: Polarized Neutron Scattering, Series "Matter and Materials", Vol. 12, Forschungszentrum Jülich, Jülich, 2002.
[8] B.P. Toperverg, Appl. Phys. A 74 (2002) S1560.
[9] B. Toperverg, O. Nikonov, V. Lauter-Pasyuk, H.J. Lauter, Physica B 297 (2001) 169.
[10] N. Mott, H.S.W. Messey, The Theory of Atomic Collisions, Clarendon Press, Oxford, 1965.
[11] G.H. Vineyard, Phys. Rev. B 26 (1982) 4146.
[12] S. Dietrich, H. Wagner, Z. Phys. B 56 (1984) 207.
[13] S.K. Sinha, E.B. Sirota, S. Garoff, H.B. Stanley, Phys. Rev. B 38 (1988) 2297.
[14] L.G. Parratt, Phys. Rev. 95 (1954) 359.
[15] E. Kentzinger, U. Rücker, B. Toperverg, Th. Brückel, in these Proceedings (PNCMI 2002), Physica B 335 (2003).
[16] B.B. Mandelbrodt, The Fractal Geometry of Nature, Freeman, New York, 1982.
[17] V. Lauter-Pasyuk, H.J. Lauter, B. Toperverg, O. Nikonov, E. Kravtsov, L. Romashev, V. Ustinov, J. Magn. Magn. Mater. 226–230 (2001) 1694.
[18] U. Rücker, E. Kentzinger, B. Toperverg, F. Ott, Th. Brückel, Appl. Phys. A 74 (2002) S607.
[19] A. Rühm, B.P. Toperverg, H. Dosch, Phys. Rev. B 60 (1999) 16073.
[20] B.P. Toperverg, A. Rühm, W. Donner, H. Dosch, Physica B 267–268 (1999) 198.